Biomaterials 289 (2022) 121802

Contents lists available at ScienceDirect

Biomaterials

journal homepage: www.elsevier.com/locate/biomaterials

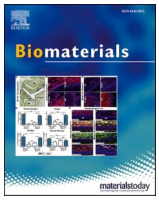

Dynamic gelatin-based hydrogels promote the proliferation and self-renewal of embryonic stem cells in long-term 3D culture

xiayi xu [a], Qian Feng [b,c], Xun Ma [d,e], Yingrui Deng [a], Kunyu Zhang [a,h], Hon Son Ooi [a], Boguang Yang [a], Zhi-Yong Zhang [f,**], Bo Feng [d,e,g,***], Liming Bian [h,i,j,k,*]

[a] Department of Biomedical Engineering, The Chinese University of Hong Kong, Hong Kong SAR, 999077, China
[b] Key Laboratory of Biorheological Science and Technology, Ministry of Education, College of Bioengineering, Chongqing University, Chongqing, 400044, China
[c] Chongqing Key Laboratory of Soft-Matter Material Chemistry and Function Manufacturing, Chongqing, 400044, China
[d] Center for Regenerative Medicine and Health, Hong Kong Institute of Science and Innovation, Chinese Academy of Sciences Limited, Hong Kong SAR, 999077, China
[e] School of Biomedical Sciences, Faculty of Medicine, Institute for Tissue Engineering and Regenerative Medicine (iTERM), CUHK-GIBH Joint Research Laboratory on Stem Cells and Regenerative Medicine, The Chinese University of Hong Kong, Hong Kong SAR, 999077, China
[f] Translational Research Centre of Regenerative Medicine and 3D Printing of Guangzhou Medical University, Guangdong Province Engineering Research Center for Biomedical Engineering, State Key Laboratory of Respiratory Disease, The Third Affiliated Hospital of Guangzhou Medical University, Guangzhou City, Guangdong Province, 510150, China
[g] Guangzhou Institute of Biomedicine and Health, Chinese Academy of Sciences, Guangzhou Regenerative Medicine and Health Guangdong Laboratory, Guangzhou, China
[h] School of Biomedical Sciences and Engineering, South China University of Technology, Guangzhou, 511442, China
[i] National Engineering Research Center for Tissue Restoration and Reconstruction, South China University of Technology, Guangzhou, 510006, China
[j] Key Laboratory of Biomedical Materials and Engineering of the Ministry of Education, South China University of Technology, Guangzhou, 510006, China
[k] Guangdong Provincial Key Laboratory of Biomedical Engineering, South China University of Technology, Guangzhou, 510006, China

A B S T R A C T

Long-term maintenance of embryonic stem cells (ESCs) in the undifferentiated state is still challenging. Compared with traditional 2D culture methods, 3D culture in biomaterials such as hydrogels is expected to better support the long-term self-renewal of ESCs by emulating the biophysical and biochemical properties of the extracellular matrix (ECM). Although prior studies showed that soft and degradable hydrogels favor the 3D growth of ESCs, few studies have examined the impact of the structural dynamics of the hydrogel matrix on ESC behaviors. Herein, we report a gelatin-based structurally dynamic hydrogel (GelCD hydrogel) that emulates the intrinsic structural dynamics of the ECM. Compared with covalently crosslinked gelatin hydrogels (GelMA hydrogels) with similar stiffness and biodegradability, GelCD hydrogels significantly promote the clonal expansion and viability of encapsulated mouse ESCs (mESCs) independent of MMP-mediated hydrogel degradation. Furthermore, GelCD hydrogels better maintain the pluripotency of encapsulated mESCs than do traditional 2D culture methods that use MEF feeder cells or medium supplementation with GSK3β and MEK 1/2 inhibitors (2i). When cultured in GelCD hydrogels for an extended period (over 2 months) with cell passaging every 7 days, mESCs preserve their normal morphology and maintain their pluripotency and full differentiation capability. Our findings highlight the critical role of the structural dynamics of the hydrogel matrix in accommodating the volume expansion that occurs during clonal ESC growth, and we believe that our dynamic hydrogels represent a valuable tool to support the long-term 3D culture of ESCs.

1. Introduction

Embryonic stem cells (ESCs), derived from the inner cell mass of early blastocysts, have the capacity to self-renew in an undifferentiated state and to differentiate into all types of adult cells [1–3]. Therefore, ESCs are highly instrumental to basic research and offer tremendous promise for biomedical applications [4–8]. Traditionally, coculture with mouse embryonic fibroblast (MEF) feeder cells or medium supplements such as GSK3β and Mek 1/2 inhibitors (2i) are needed for routine 2D culture of ESCs to inhibit spontaneous differentiation [9–12]. Nevertheless, maintaining ESCs in the undifferentiated state in long-term culture is still challenging [13–15]. More importantly, unlike ESCs cultured on 2D substrates *in vitro*, during embryonic development, ESCs in the inner cell mass interact with the 3D extracellular matrix (ECM),

* Corresponding author.
** Corresponding author.
*** Corresponding author.
E-mail addresses: summerincuhk@gmail.com (xu), mr.zhiyong@gmail.com, drzhiyong@126.com (Z.-Y. Zhang), fengbo@cuhk.edu.hk (B. Feng), bianlm@scut.edu.cn (L. Bian).

https://doi.org/10.1016/j.biomaterials.2022.121802
Received 29 June 2022; Received in revised form 12 August 2022; Accepted 9 September 2022
Available online 13 September 2022

and this interaction regulates self-renewal and differentiation of ESCs [16]. The interaction between cells and the surrounding ECM is of vital importance for cell proliferation, maintenance, differentiation, and organogenesis [17]. 3D biomaterial scaffolds, such as hydrogels, are expected to facilitate the long-term growth of ESCs in the absence of feeder layers without the need for frequent subculturing [18].

Hydrogels, which resemble the hydrated polymeric architecture of the ECM, have been explored for 3D culture of ESCs in several studies [19–31]. Previous studies demonstrated the utility of hydrogels to support the expansion, pluripotency maintenance, directed differentiation, and model aspects of embryogenesis (such as epiblast-like morphological formations) of ESCs [19–23]. Several studies have shown that a soft hydrogel matrix with low stiffness favors the growth of mESC colonies while the underlying mechanism is still unclear [24,25]. Nevertheless, while there have been numerous studies on the development of structurally dynamic hydrogels to study the cell-hydrogel interactions of adult stem cells such as human mesenchymal stem cells (hMSCs) [26–30], few studies have closely examined the impact of hydrogel matrix structural dynamics on ESC functions. It should be noted that the effect of matrix dynamics on cells differs greatly under different circumstances towards stem cells. For example, the structural dynamics originating from hydrogel degradation were reported to promote hMSCs differentiation towards osteogenesis by enhancing mechanotransduction signaling [31]. In contrast, matrix metalloproteinase (MMP)-degradable poly (ethylene glycol) (PEG) hydrogels better supported the proliferation and pluripotency of mouse ESCs (mESCs) than did nondegradable PEG hydrogels [23,24].

To emulate the intrinsic structural dynamics of the ECM that are derived from its physical crosslinks [29], the incorporation of reversible crosslinks has been extensively investigated to develop cell-adaptable dynamic hydrogels [32–36]. Unlike degradable hydrogels, dynamic hydrogels based on intrinsically reversible crosslinks are spatially and temporally consistent [29]. Such hydrogels provided a permissive and spatiotemporally consistent 3D matrix to allow systematic investigation of the impact of hydrogel network dynamics on cells free of the confounding factors associated with degradable hydrogels. For example, Chaudhuri et al. showed that the fast stress relaxation properties of alginate hydrogels crosslinked by ions promoted mechanosensing and osteogenic differentiation in hMSCs [35]. Our previous work also showed that gelatin-based host-guest dynamic hydrogels promoted the 3D spreading and osteogenesis of hMSCs [37,38]. In addition, gelatin is used as the standard coating matrix for the 2D culture of mESCs to aid in attachment [39]. So far, very few studies have examined the effect of dynamic hydrogels on the proliferation and stemness maintenance of ESCs [40]. Indana et al. used a viscoelastic alginate-based hydrogel to study human induced pluripotent stem cells (hiPSC) morphogenesis in 3D culture. This study showed that fast stress relaxation promoted hiPSC viability and proliferation while slow stress relaxation triggered hiPSC apoptosis [40]. In this work, we evaluated the efficacy of our gelatin-based dynamic hydrogel in supporting the 3D clonal expansion and pluripotency of ESCs during long-term culture.

In this study, we fabricated gelatin-based dynamic hydrogels (GelCD hydrogels) crosslinked by supramolecular interactions between cyclodextrin and aromatic residues of gelatin. We demonstrated that compared with covalently crosslinked GelMA hydrogels with similar stiffness and biodegradability, the GelCD hydrogels significantly promoted clonal expansion and better maintained the pluripotency of the encapsulated mESCs in 3D culture. Furthermore, mESCs cultured in GelCD hydrogels maintained pluripotency during long-term culture better than mESCs obtained from traditional 2D culture methods that used MEF feeder cells or medium supplemented with inhibitors (2i). After more than 2 months of long-term 3D culture in the GelCD hydrogels with regular cell retrieval and passaging every 7 days, mESCs were still capable of differentiation into three germ layers. Inhibition of MMP-mediated hydrogel degradation did not affect the enhanced clonal expansion of mESCs in the GelCD hydrogels, indicating the critical role of the intrinsic dynamics of the GelCD hydrogel network in supporting mESC expansion in 3D culture. We believe that the covalently crosslinked static network of GelMA hydrogels hinders the development of mESC colonies, whereas the reversibly crosslinked dynamic network of GelCD hydrogels can accommodate substantial volumetric expansion during the clonal expansion of mESCs and better maintain mESC pluripotency. Our findings highlight the importance of the structural dynamics of the hydrogel 3D matrix for the 3D culture of ESCs, and our dynamic hydrogels can be a valuable tool to support the long-term 3D culture of ESCs.

2. Results and discussion

2.1. GelCD hydrogels demonstrated dynamic properties derived from reversible host-guest complexation

We fabricated dynamic gelatin host–guest hydrogels based on the method reported in our previous works [41]. Briefly, acryloyl beta-cyclodextrin (ac-β-CD) with an average acryloyl substitution degree (SD) of 1.0 was synthesized (Fig. S1) and used as the host monomer to complex with aromatic residues (e.g., phenylalanine, tyrosine and tryptophan) in gelatin via the reversible host–guest complexation [42–44] (Fig. 1a). The subsequent photo-polymerization of the obtained self-assembled gelatin–CD complex produced the host–guest hydrogels (GelCD hydrogels) [38] (Fig. 1b). To demonstrate the effect of reversible host–guest crosslinks on the growth and self-renewal of mESCs in GelCD hydrogels, we also fabricated covalently crosslinked methacryloyl gelatin (GelMA) hydrogels via photo-polymerization [45] (Fig. 1b). To decouple the effect of the hydrogel stiffness, which was reported to influence the growth of encapsulated mESCs [24,25], we fabricated GelMA hydrogels with stiffnesses identical to (GelMA-1, $G' = 912$ Pa) and higher than (GelMA-2, $G' = 5886$ Pa) that of GelCD hydrogels (Fig. 1c and Fig. S3). Tuning of GelMA hydrogel stiffness was achieved by adjusting the degree of methacryloyl substitution (Fig. S2) [46]. The higher G'' of GelCD hydrogels than GelMA-1 hydrogels indicated a higher level of network dynamics in GelCD hydrogels. We purposely fabricated GelCD and GelMA-1 hydrogels with relatively high stiffness, which has been reported to impede the colony growth of encapsulated mESCs [23,24], so that we could evaluate the effect of the dynamic network of GelCD hydrogels on the growth of encapsulated mESCs. In addition to stiffness, previous studies also reported that degradation of hydrogels is an important parameter for regulating mESC growth in hydrogels [23,24]. Previous studies showed that the biodegradation of gelatin-based hydrogels depends on the concentration of gelatin (kept at 8% w/v for all hydrogels in this study) and the bulk mechanical strength of the hydrogels [47]. The GelCD and GelMA-1 hydrogels showed similar degradation rates in the presence of 1 mg/mL collagenase (type II) at 37 °C, while the degradation rate of GelMA-2 hydrogels under the same conditions was much slower (Fig. 1d). By using the GelMA-1 hydrogels as the control group, we can decouple the effects of stiffness and degradation of the hydrogels from that of the dynamic network of GelCD hydrogels on the growth of encapsulated mESCs.

The dynamic properties of the GelCD hydrogels were further investigated. Oscillatory frequency-sweep rheological tests revealed that the G' value of the GelCD hydrogels is frequency-dependent, whereas the G' value of the GelMA-1 and GelMA-2 hydrogels showed no frequency dependence (Fig. 1e). We next evaluated the half stress relaxation time ($\tau_{1/2}$) of the hydrogels, which is defined as the time at which the stress declines to 50% of its initial value under constant compressive strain [27]. The GelCD hydrogels showed a significantly shorter half stress relaxation time ($\tau_{1/2} = 40.2$ s) than static GelMA-1 hydrogels ($P < 0.0001$, $\tau_{1/2} = 415.4$ s) and GelMA-2 hydrogels ($P < 0.0001$, $\tau_{1/2} = 768.3$ s) (Fig. 1f and g). Additionally, the physical associations among gelation chains are believed to contribute to the stress relaxation of the covalently crosslinked GelMA hydrogels. Furthermore, the GelCD hydrogels underwent a transition between “sol” and “gel” under

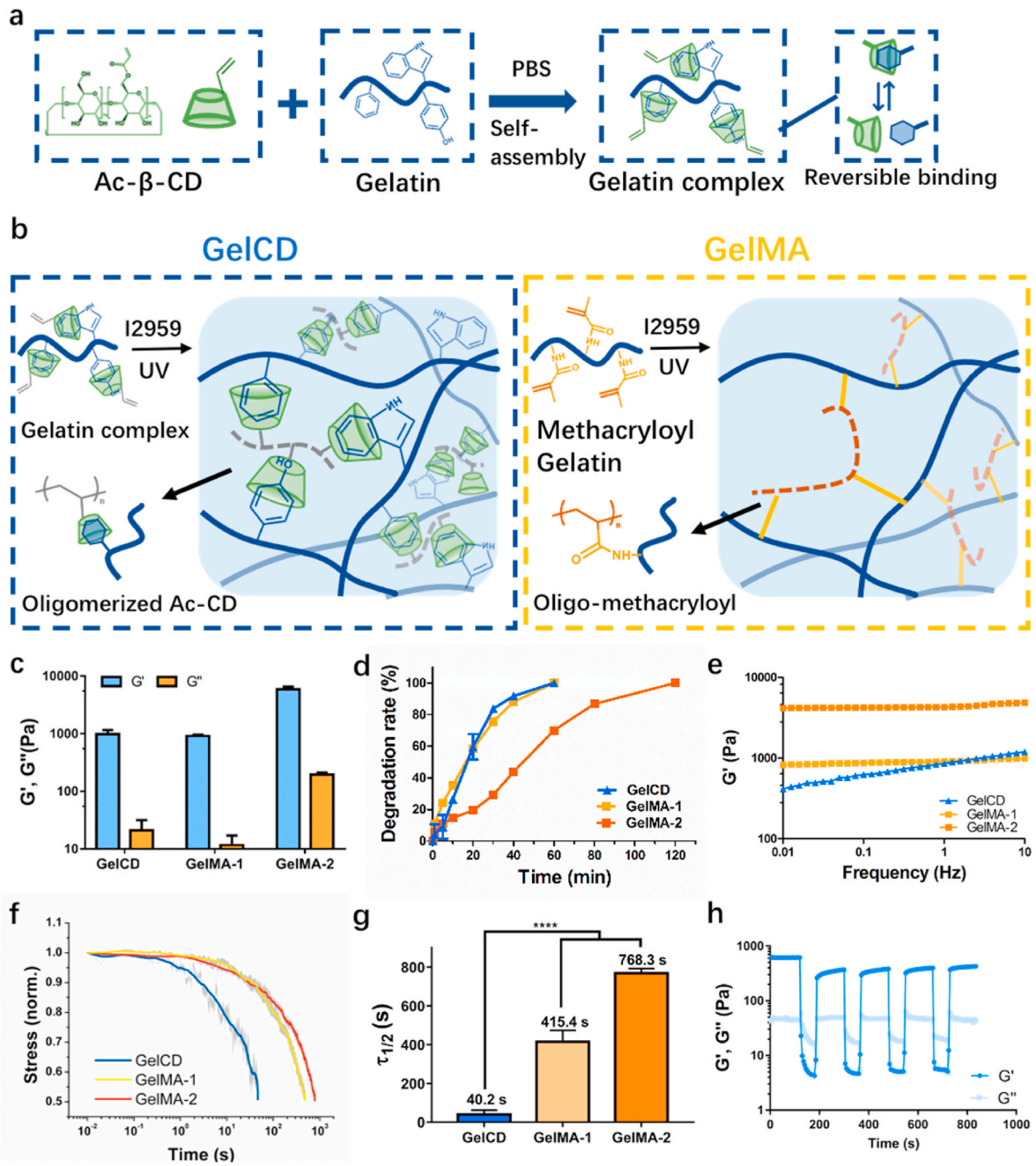

Fig. 1. (a) Schematic illustration of the self-assembly of ac-β-CD and aromatic residues of gelatin and the resultant gelatin–CD complex based on reversible host-guest complexation as the precursor of GelCD hydrogels. **(b)** Schematic illustration of dynamic host-guest crosslinking structure of the GelCD hydrogels where gray dash line represents the crosslinking of adjacent ac-CD monomers, and the covalent crosslinking of GelMA hydrogels where brown dash line represents the crosslinking of adjacent methacryloyl groups. **(c)** The average storage (G′) and loss (G″) moduli collected from three independent parallel time sweep tests of GelCD, GelMA-1, and GelMA-2 hydrogels. N = 3 (materials replicates). **(d)** The degradation rate of the hydrogels in the presence of 1 mg/mL collagenase (type II) at 37 °C. n = 3 (materials replicates). The determination of the degradation rate was showed in Materials and methods. **(e)** The G′ of GelCD and GelMA hydrogels from frequency sweep tests which were recorded at a fixed strain of 0.1% and a changing frequency from 0.01 to 10 Hz. **(f)** Stress relaxation test for hydrogels crosslinked by dynamic or covalent bonds (15% peak compressive strain). **(g)** $\tau_{1/2}$ (at which the stress is relaxed to half of the peak stress) of different hydrogels, including GelCD, GelMA-1 and GelMA-2 hydrogels. N = 3 (materials replicates). **(h)** The dynamic GelCD hydrogels underwent a "sol-gel" transition under alternating high (500%) and low (1%) shear strains at 37 °C. ****P < 0.0001. (For interpretation of the references to color in this figure legend, the reader is referred to the Web version of this article.)

alternating high (500%) and low (1%) shear strains, respectively. The G′ value almost fully recovered to the initial level instantaneously as the hydrogels returned to the "gel" state (Fig. 1h). The observed fast relaxation, shear-thinning, and self-healing behaviors of GelCD hydrogels confirmed the reversible and dynamic crosslinking structures of the GelCD hydrogels, which enabled network rearrangement under mechanical loading [38]. We expect that the dynamic host-guest crosslinked network of the GelCD hydrogel, which is not found in the covalently crosslinked GelMA hydrogels, will better accommodate the dramatic volume expansion of growing mESC colonies in the hydrogels.

2.2. Dynamic GelCD hydrogels better support the clonal expansion of encapsulated mESCs

To encapsulate mESCs in the hydrogels, mESCs were suspended in the hydrogel precursor solutions before UV-induced gelation (detailed information is shown in the methods). A previous study found that long-term (4 h) UV exposure caused DNA damage and p53 protein accumulation in the nuclei of ESCs [48]. However, we found that mESCs exposed to 10 min of UV light at the low intensity used in this study showed the same minimal p53 expression as cells that were not exposed to UV (Fig. S4). This result suggested that the short exposure (10 min) to low-intensity UV light (10 mW/cm^2) used for photo-gelation did not induce significant damage to the DNA of encapsulated mESCs. After encapsulation in the hydrogels (1.5×10^5 cells per 50 μl hydrogel), individual mESCs were uniformly distributed throughout the hydrogels (Fig. 2a). In the following 7 days of culture in MEF-conditioned medium containing LIF and mESC-specific serum, the mESCs in the GelCD hydrogels developed into significantly larger spherical colonies than those in the GelMA-1 and GelMA-2 hydrogels (Fig. 2b, cross-sectional area, GelCD: 15,557 μm^2 vs. GelMA-1: 1066 μm^2 vs. GelMA-2: 265 μm^2 at day 7). The encapsulated mESCs in the GelMA-2 hydrogels barely proliferated and remained as single cells during 7 days of culture (Fig. 2a and b).

Live/dead staining further indicated that most mESCs in the GelCD hydrogels remained viable (green) with very limited apoptotic events (red) during the 7 days of culture (Fig. 2a). However, the viability of mESCs in the GelMA-1 hydrogels decreased dramatically with increasing culture time, and there were only dead cells in the colonies at day 7. Consistent with the bright-field images, the majority of mESCs in the GelMA-2 hydrogels remained as isolated single cells, with increasing dead cells over time (Fig. 2a, Fig. S5). To further examine the cell viability of mESCs in hydrogels, flow cytometry analysis of cells stained with both Annexin V-FITC and 7-AAD was performed. The early apoptosis of cells can be detected by Annexin V-FITC staining, while necrotic cells can be detected by 7AAD staining due to its permeability in damaged cell membranes [49]. The results showed that after 3 days of culture, most mESCs (84.25%) were viable in GelCD hydrogels with a very low death rate (3.1%). The percentages of live cells were significantly smaller in the GelMA-1 ($P < 0.0001$) and GelMA-2 ($P < 0.0001$) groups than in the GelCD group. The GelMA-2 group showed significantly larger percentages of apoptotic cells and dead cells than the GelMA-1 group did (apoptotic cell rate: $P < 0.001$, dead cell rate: $P < 0.05$, Fig. 2c, Fig. S6). The rapid increase in colony size and long-term cell viability indicated that the GelCD hydrogels can effectively support the proliferation of encapsulated mESCs. The results of the EdU assay showed that there were significantly more proliferating cells in the single cell-derived colonies in the GelCD hydrogels than in the GelMA hydrogels during 7 days of culture (Fig. 2d and e). The fraction of proliferating cells was even smaller in GelMA-2 hydrogels than in GelMA-1 hydrogels, which is likely due to the denser covalent crosslinking of GelMA-2 hydrogels.

2.3. Dynamic GelCD hydrogels maintain the pluripotency of encapsulated mESCs independent of degradation

We speculated that while the dense covalent crosslinks in GelMA-1 hydrogels severely restricted the growth of mESC colonies, the cell-mediated degradation of GelMA-1 hydrogels enabled a slight increase in the mESC colony size. On the other hand, the dynamic host–guest crosslinks in the GelCD hydrogels, rather than hydrogel degradation, played a vital role in supporting the clonal growth and self-renewal of encapsulated mESCs (Fig. 3a). To verify this hypothesis, we first evaluated the dynamic property of GelCD hydrogels with mESC encapsulation. The results showed that there was no significant difference between the $\tau_{1/2}$ of GelCD hydrogels with ($\tau_{1/2} = 40.2$ s) or without ($\tau_{1/2} = 40.3$ s) mESCs encapsulation ($P > 0.05$, Fig. S7). An MMP inhibitor (GM 6001, final concentration: 50 μM) was supplemented to the culture medium to suppress cell-mediated hydrogel degradation. The results showed that mESCs remained as isolated single cells on day 7 with significantly reduced expression of stemness markers of NANOG ($P < 0.0001$) and OCT3/4 ($P < 0.01$) (Fig. 3b and c). In contrast, the robust colony growth and the NANOG and OCT3/4 expressions of mESCs in the GelCD hydrogels were barely affected by the MMP inhibitor treatment and remained similar to that of the untreated mESCs in the GelCD hydrogels (NANOG, OCT3/4: $P > 0.05$) (Fig. 3b and c). To further evaluate the effect of MMP inhibitor treatment on mESCs proliferation in GelCD and GelMA-1 hydrogels, EdU staining was performed after 7 days of MMP inhibitor treatment. MMP inhibition treatment completely abolished the proliferation of mESCs in GelMA-1 hydrogels as indicated by significantly reduced EdU-positive cells ($P < 0.0001$, Fig. 3d and Fig. S8). In contrast, consistent with the previous findings, the MMP inhibitor treatment did not significantly decrease the fraction of EdU-positive cells in the GelCD hydrogels ($P > 0.05$) (Fig. 3d and Fig. S8). This result further confirmed that the mESCs proliferation in GelCD hydrogels is independent of MMP-mediated hydrogel degradation.

These results suggest that given similar bulk stiffnesses and biodegradation rates, the dynamic GelCD hydrogels better supported the clonal expansion and stemness maintenance of encapsulated mESCs than the covalently crosslinked static GelMA hydrogels. Increasing the covalent crosslinking density in the GelMA hydrogels further inhibited the proliferation of encapsulated mESCs. Inhibition of MMP-mediated gelatin degradation did not significantly influence the proliferation and pluripotency of mESCs in the GelCD hydrogels but abolished the limited growth of mESCs in the GelMA hydrogels with stiffness similar to that of GelCD hydrogels.

Previous studies have shown that many cell types can maintain high viability for several days in GelMA hydrogels [46,50–52], and we have also tested the viability of hMSCs and 3T3 cells during 7-days of 3D culture in GelMA hydrogels. Both hMSCs and 3T3 cells encapsulated in GelMA-1 and GelMA-2 hydrogels showed significant increase in alamarBlue reading from day 1 to day 7, indicating excellent viability of both cell types in GelMA hydrogels (Fig. S9a). Meanwhile, live/dead staining at day 7 also revealed that most of the hMSCs and 3T3 in GelMA-1 (hMSCs: ~96.6%; 3T3: ~91.0%) and GelMA-2 (hMSCs: ~92.4%; 3T3: ~90.6%) hydrogels remained viable after 7 days of culture (Figs. S9b and c), thereby confirming the cytocompatibility of GelMA hydrogels used in this study. These results also indicated that the nutrient and oxygen transport within GelMA hydrogels is sufficient to support cell growth and is not the reason for the poor growth mESCs in GelMA hydrogels. To demonstrate general applicability of GelCD hydrogels for mESC culture, we also tested another two sources of mESCs, the results showed that similar to the results obtained using E14 mESCs, both D3 mESCs and a self-validated mESC line [53] encapsulated in GelCD hydrogels can proliferate very well during 7-days of culture and grew into large colonies with strong expression of pluripotent markers (NANOG and OCT3/4) (Fig. S10). Therefore, the intrinsically dynamic network of GelCD hydrogels can provide a more permissive pericellular microenvironment to accommodate the substantial volumetric expansion that occurs during mESC proliferation and maintain pluripotency independent of major hydrogel degradation.

2.4. Dynamic GelCD hydrogels promote long-term self-renewal of mESCs compared with conventional 2D culture methods

We first confirmed that compared with the 2D culture of mESCs on the GelCD hydrogel surface, the 3D encapsulation of mESCs in the GelCD hydrogels promoted proliferation and stemness maintenance of mESCs (Fig. S11 and Fig. S12). Next, we further assessed the efficacy of the GelCD hydrogels in supporting the expansion of mESCs in 3D cultures by benchmarking with two conventional 2D culture methods, which employ MEF feeder cells (MEFs) or inhibitors of GSK3β and MEK 1/2 (2i). MEF-conditioned medium without 2i supplements was used for

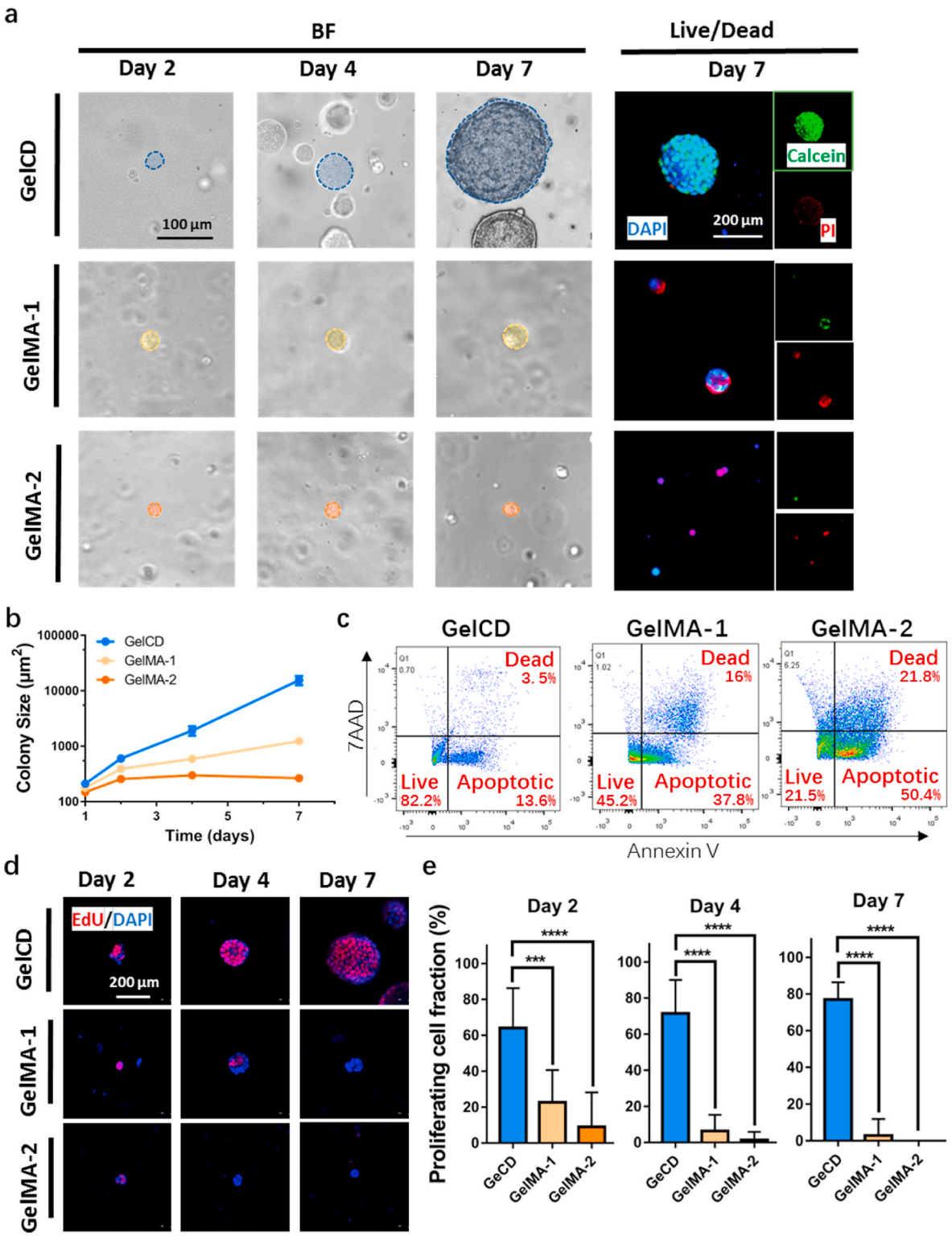

Fig. 2. (a) Representative bright-field images at days 2, 4, and 7 and live/dead staining images at day 7 of mESCs encapsulation in GelCD and GelMA hydrogels. In each image, a representative colony was colored to show the growth of mESCs. **(b)** The colony growth of mESCs in GelCD and GelMA hydrogels during 7 days of culture evaluated by the maximal cross-sectional area of the colonies. N = 10 (biological replicates). **(c)** Flow cytometry results on day 7 for mESCs stained with both Annexin V and 7-AAD to quantify the viability of mESCs in hydrogels. **(d)** EdU staining of mESC colonies in GelCD, GelMA-1, and GelMA-2 hydrogels, where positive staining indicated proliferating cells. **(e)** The percentages of EdU-positive cell nuclei among all cell nuclei per high-power field (HPF). N = 10 (biological replicates), ***P < 0.001, ****P < 0.0001.

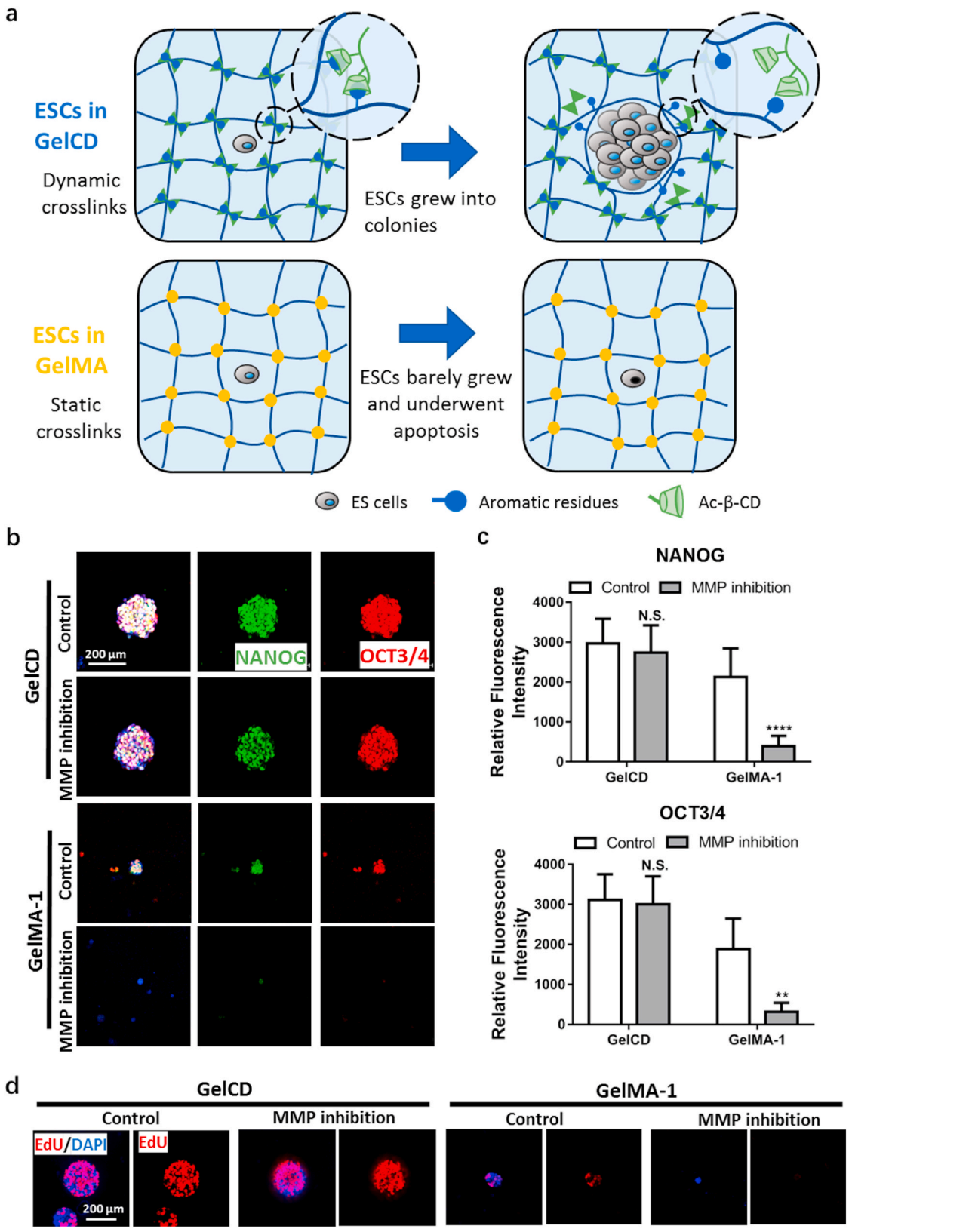

Fig. 3. (a) Schematic illustration of the hypothesis that the dynamic network of GelCD hydrogels can accommodate the substantial volumetric expansion associated with mESC colony growth, while the static and dense covalent crosslinks in GelMA hydrogels restrict the growth of mESC colonies. (**b**) Immunostaining for the stemness markers NANOG and OCT3/4 in mESC colonies in the GelCD and GelMA-1 hydrogels with or without MMP inhibitor treatment. **(c)** Quantification of the relative fluorescence intensity of NANOG and OCT3/4 staining in each colony in hydrogels. N = 10 (biological replicates). **(d)** EdU staining of mESC colonies in GelCD and GelMA-1 hydrogels with or without MMP inhibitor treatment, where positive staining indicates proliferating cells. N. S. in (c) is the abbreviation of "not significant". $^{N.S.}P > 0.05$, $^{**}P < 0.01$, $^{****}P < 0.0001$.

mESC culture in GelCD hydrogels. Although the average maximal cross-sectional area of 3D mESC colonies in the GelCD hydrogels was smaller than that of 2D mESC colonies obtained by using MEF or 2i method in the first 4 days, the colony size became comparable among the three groups on day 7 (Fig. 4a and b). It should be noted that the mESC colonies developed in the GelCD hydrogels were 3D spheroids and should therefore contain more cells than the mESC colonies of similar size developed from the 2D culture methods, which had a relatively flat morphology [54]. The 3D mESC colonies in the GelCD hydrogels were spherical and compact, whereas mESC colonies generated via the 2D methods were irregularly shaped (Fig. 4a). These observations were confirmed by quantitative analysis of the morphology and geometry of the mESC colonies in each group. Both the circularity and aspect ratio of mESC colonies in the GelCD hydrogels were significantly closer to 1 than those in 2D culture groups at days 2, 4 and 7 (Fig. 4c and d). Notably, in the MEF and 2i groups, there was a significant increase in the aspect ratio and a dramatic decrease in circularity on day 7. This is consistent with previous findings that ESCs underwent differentiation on rigid 2D substrates during long-term culture [55,56]. At day 7, the colonies in 2D cultures showed a very loose cell aggregate structure. And the cells at the edge of the colonies exhibited a spreading filamentous actin structure and weak expression of the stemness marker SOX2. This is an indication of differentiation of these cells. In contrast, the colonies in GelCD hydrogels maintained their spherical cortex actin arrangement with high SOX2 expression at day 7 (Fig. 4e).

The pluripotency of mESCs in different groups was further examined. The immunofluorescence staining results showed that the mESCs exhibited substantial expression of pluripotency markers including NANOG and OCT3/4 over 7 days, while the expression of NANOG and OCT3/4 in the MEF and 2i groups diminished significantly after only 2 days of culture. This is consistent with the need to passage mESCs every 2 days for both the MEF and 2i methods to maintain ESC pluripotency (Fig. 5a and b). Consistent with the immunostaining results, the qPCR results also showed significantly higher expression levels of SOX2, NANOG, and OCT3/4 in the GelCD group than in the 2i and MEF groups at day 7 (Fig. 5c).

To further evaluate the efficacy of GelCD hydrogels in maintaining the pluripotency of encapsulated mESCs during long-term 3D culture, we continued to culture mESCs in GelCD hydrogels for 2 months. During the 2-month culture, the cultured cells were retrieved from GelCD hydrogels using collagenase and immediately re-encapsulated in freshly prepared GelCD hydrogels every 7 days. After 9 times of cell passaging in GelCD hydrogels, the mESCs still formed tight and well-defined spherical colonies with strong expression of NANOG and OCT3/4 in GelCD hydrogels. The UV irradiation at low intensity (10 mW/cm) was applied for only 10 min to induce photo-gelation at every 7 days during the two-month long culture. Several studies have reported the safe use of UV irradiation at similar dosage to induce hydrogel gelation or degradation for ESC culture [18,19,21,57]. Therefore, we consider the dosage of UV used in our study cytocompatible. The mESCs retrieved from the GelCD hydrogels still formed tight and well-defined colonies with robust immunofluorescence staining for nuclear NANOG and OCT3/4 in the same manner as the mESCs passaged routinely on MEFs (Fig. S13). The retrieved mESCs were also cultured in suspension to evaluate the spontaneous differentiation of mESCs and the formation of embryonic bodies (EBs) (procedure shown in Fig. S14). Nestin-positive, α-fetoprotein-positive, and α-SMA-positive cells representing differentiated cells of all three germ layers [19,58–60] can all be found in the formed EBs, indicating functional pluripotency of mESCs obtained after 2 months of 3D culture in the GelCD hydrogels (Fig. 5d). These findings together demonstrate that the GelCD hydrogel is an effective 3D culture platform for supporting the proliferation and self-renewal of mESCs in long-term culture without using feeder cells or 2i supplements in the medium.

The migration, spreading and proliferation of cells and the expansion of colonies and organoids in 3D matrices, such as the hydrogel network, usually require degradation or physical remodeling of the hydrogel network for the cells to overcome the spatial confinement. On the other hand, the spatial confinement of static hydrogels greatly limits the cellular volumetric expansion [61–65]. The capability of cells to adapt hydrogel network is of high importance for cell division and proliferation. It was reported that for cells at metaphase entrapped in stiff hydrogels with slow stress relaxation, most cells did not progress through mitosis and the failure of cell division led to cell apoptosis [66]. To promote the growth of cell colonies and organoids in hydrogels, researchers generally employ protease-degradable hydrogels to accommodate the volumetric expansion of growing colonies and organoids in the hydrogels [63–65,67]. ESCs have a much shorter cell cycle (around 12 h) and therefore more rapid proliferation than hMSCs and 3T3, which require timely adaptation of the surrounding hydrogel network when cultured in 3D hydrogels [68]. In this study, the spatial confinement of the rigid covalently crosslinked and slow degrading network of GelMA hydrogels may have restricted the proliferation of encapsulated mESCs, thereby leading to the rapid apoptosis of mESCs as evidenced by the significantly elevated PI staining and decreasing Calcein AM staining after only 2 days (Fig. S5). In contrast, the intrinsically dynamic network of GelCD hydrogels better support the rapid proliferation of the encapsulated mESCs. Our findings are consistent with the previous work in which alginate-based hydrogels with tunable stress relaxation were used to study hiPSC growth in 3D culture [40]. Our study employed a different structurally dynamic hydrogel based on the host–guest complexation, and we demonstrated that the supramolecular hydrogel can promote the proliferation and maintain the stemness of ESCs in 3D culture over 2 months, while this is challenging for the conventional culture methods.

Our study has several limitations. Although we successfully examined that dynamic hydrogel can better support the growth of mouse embryonic stem cells, hESCs did not proliferate as well in the our GelCD hydrogel. Previous studies have indicated that hESCs are drastically different from mESCs in terms of development stage and many other aspects [69,70]. We have been examining the different requirements for sustaining hESCs in 3D matrix and developing other dynamic hydrogels that can be applicable to supporting both mouse and human pluripotent stem cells. Besides, we used simple spontaneous differentiation experiments to quickly confirm the pluripotency of the cultured mESCs. In the next step, we would also like to comprehensively study how the matrix dynamic direct the ESC differentiation and embryonic development. More importantly, together with the previous report [40], hydrogel matrix dynamic is critical to both growth of mESCs and hiPSCs. However, the underlaying mechanism needs to be further elucidated.

3. Conclusion

In this work, we presented a structurally dynamic hydrogel with physical crosslinking that enhanced the expansion and pluripotency maintenance of mESCs in 3D culture compared with those of conventional hydrogels with low stress relaxation or conventional 2D culture methods. The dynamic network caused by the reversible host-guest crosslinking in our GelCD hydrogels can accommodate the volumetric expansion associated with 3D ESC clonal growth. Compared to covalently crosslinked GelMA hydrogels with similar stiffness and degradability, GelCD hydrogels significantly promoted mESC colony growth and pluripotency maintenance independent of MMP-mediated hydrogel degradation. Furthermore, GelCD hydrogels can maintain the stemness of mESCs for more than 2 months without the need for frequent subculturing, which is necessary for traditional 2D culture methods. In the absence of feeder layers and 2i supplementation, mESCs cultured in GelCD hydrogels can preserve their normal morphology and maintain their undifferentiated status and full differentiation capability during long-term culture, whereas 2D culture methods cannot achieve these desired outcomes. Our findings not only demonstrate that dynamic hydrogels with physical crosslinks represent a promising platform to support long-term 3D culture of ESCs but also provide insights into the

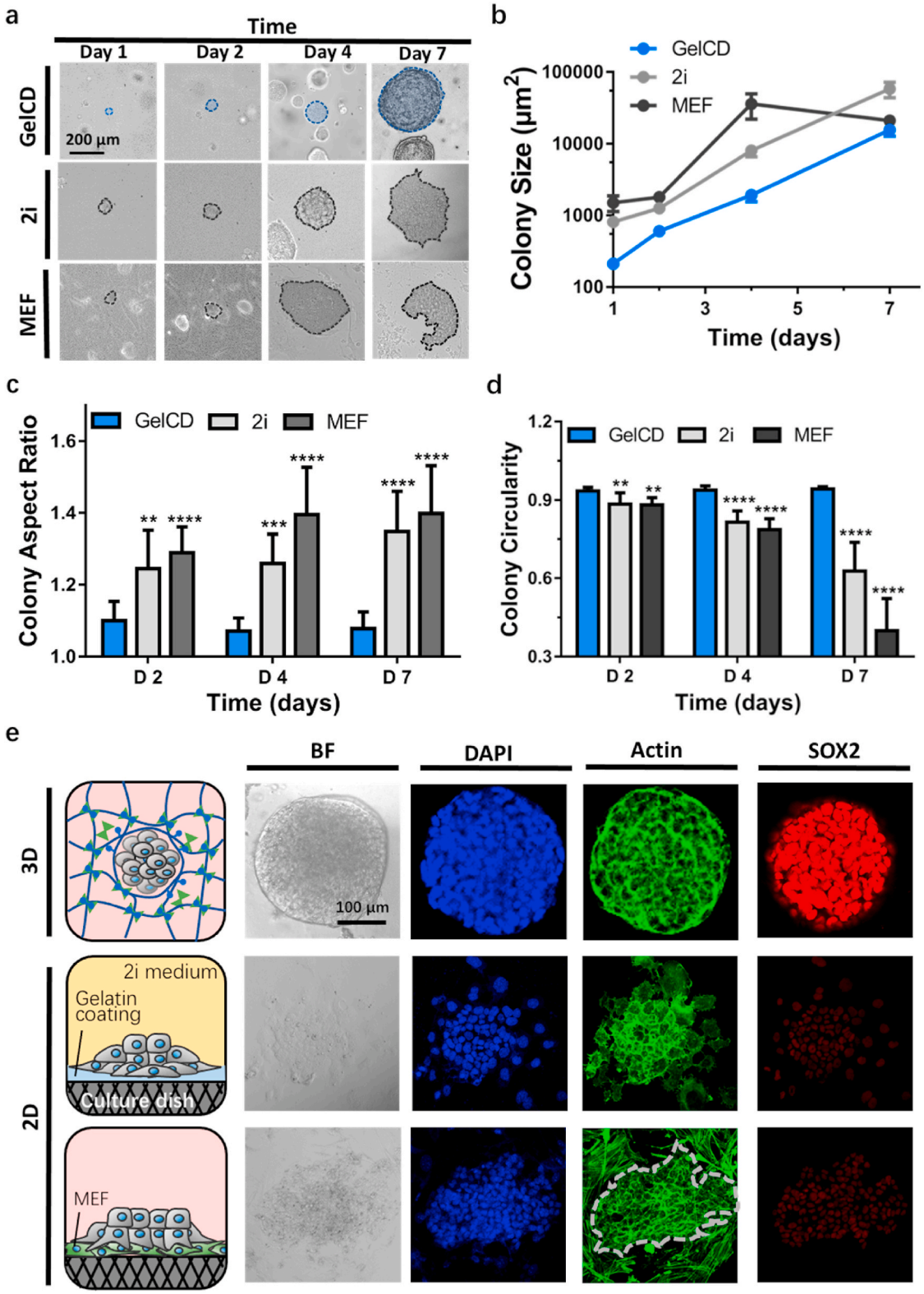

Fig. 4. (a) Representative bright-field images of mESCs encapsulated in GelCD hydrogels or cultured on 2D gelatin coated culture dishes or MEFs at days 1, 2, 4, and 7. In each image, a representative colony was colored to show the growth of mESCs. **(b)** The colony growth of mESCs in the GelCD hydrogel, 2i, and MEF groups during 7 days of culture evaluated by the maximal cross-sectional area of the colonies. N = 10 (biological replicates). The **(c)** aspect ratio and **(d)** circularity of typical mESC colonies randomly selected at days 2, 4 and 7 in each group. N = 10 (biological replicates). **(e)** Bright-field images of single colonies and immunostaining for SOX2 and F-actin on day 7. The 3D mESC colonies formed in GelCD hydrogels showed spherical and compact structures with high stemness, while the 2D colonies formed on 2D substrates (2i or MEF) exhibited a spreading morphology and low stemness. For the MEF group, green staining inside the gray dashed line indicates F-actin in ESCs, while green staining outside the gray dashed line indicates F-actin in feeder cells. $^{**}P < 0.01$, $^{****}P < 0.0001$. (For interpretation of the references to color in this figure legend, the reader is referred to the Web version of this article.)

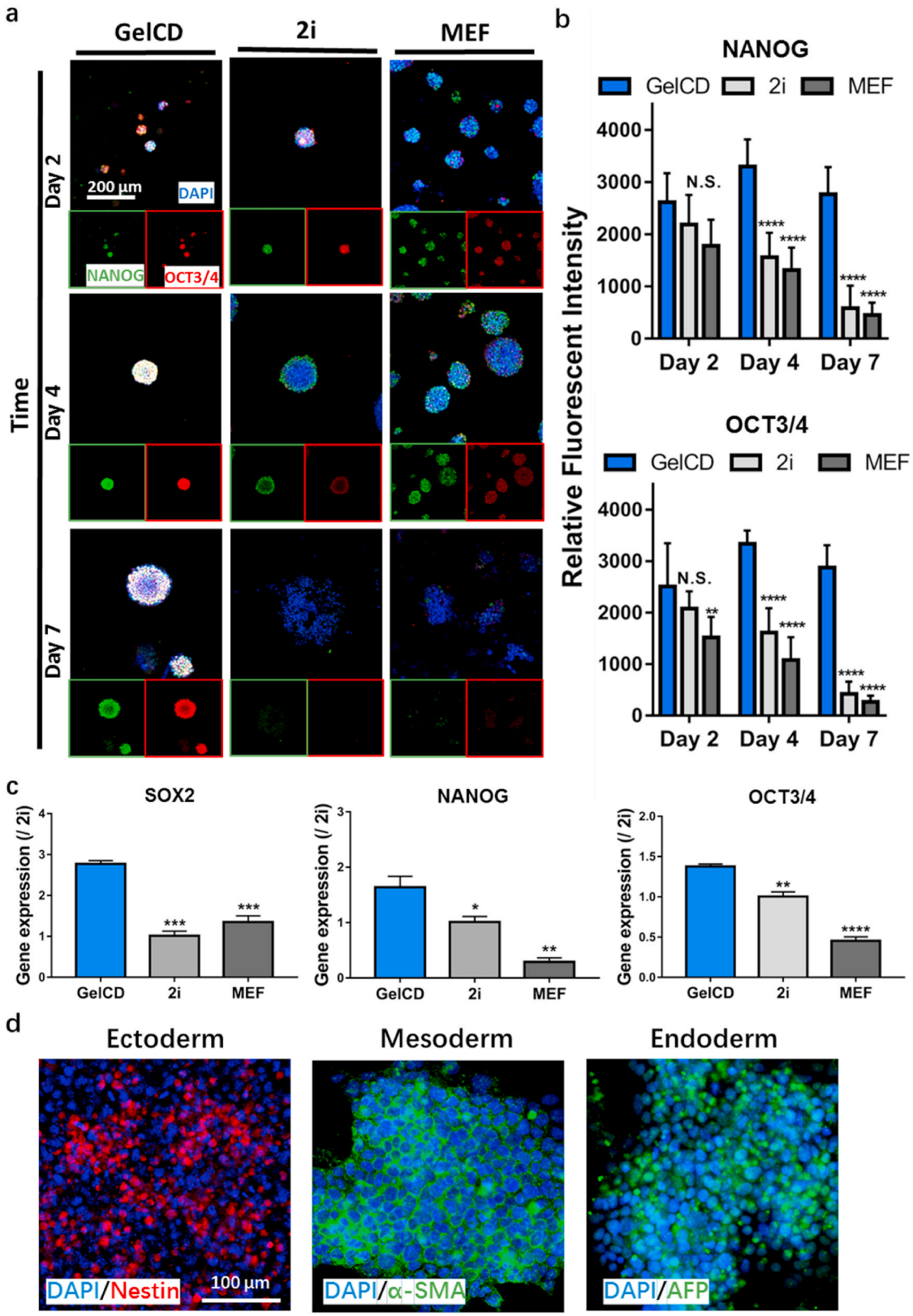

Fig. 5. (a) Immunostaining for the stemness markers NANOG and OCT3/4 in mESC colonies encapsulated in GelCD hydrogels or cultured on 2D substrates using the 2i or MEF method. **(b)** Quantification of the relative fluorescence intensity of NANOG and OCT3/4 in mESC colonies in the three groups. N = 10 (biological replicates). **(c)** qPCR quantification of SOX2, NANOG and OCT3/4 expression in mESCs in the GelCD, 2i and MEF groups. N = 3. **(d)** Immunostaining for differentiation markers related to the three germ layers in EBs formed by mESCs obtained after 2 months of long-term culture in GelCD hydrogels (Nestin: ectoderm, α-smooth muscle actin: mesoderm, and α-fetoprotein: endoderm). *P < 0.05, **P < 0.01, ***P < 0.001, ****P < 0.0001.

impact of the biophysical properties of the 3D microenvironment on ESC behaviors.

4. Materials and methods

4.1. Synthesis of acryloyl β-cyclodextrin (ac-β-cd)

10 g β-CD (Aladdin) was added into 150 mL dimethyl formamide (DMF, Fisher Scientific) before 7 mL triethyl amine (TEA, Sigma) was added into the solution. The mixture was put into ice box and the temperature of the solution was controlled around 0 °C. After adding 5 mL of acrylic acid into the solution, the mixture was continuously stirred for 12 h at around 0 °C. Afterwards, a clear solution was obtained by filtrating the mixture to remove the precipitate. Vacuum rotary evaporation method was used to concentrate the obtained clear solution to 10% of original volume. Then the concentrated solution was added slowly into large volume of acetone (for example, 10x) to precipitate the product of ac-β-CD under room temperature. The product was washed 3 times with acetone and dried thoroughly by vacuum. The acryloyl substitution degree (DS) of Ac-β-CD was estimated to be 1.0 by 1H NMR (Bruker Advance 400 MHz spectrometer) (Fig. S1).

4.2. Synthesis and characterization of methacryloyl gelatin (GelMA)

Firstly, 10% gelatin solution was prepared by dissolving gelatin (type A, from porcine skin, isoelectric point: 7–9, Cat. No, G1890-500G, Sigma) in Dulbecco's phosphate buffered saline (DPBS, Gibco) at 50 °C. Methacrylic anhydride (MA, Sigma) was then added with the final concentrations of MA as 0.1% and 10% (v/v) separately. The mixture was allowed to react for 3 h at 50 °C under stirring. The resulted GelMA solution was dialyzed against DI water using 12–14 kDa cut-off dialysis membrane at least 3 time per day for 7 days at 45 °C to remove unreacted reagent. Finally, the solution was frozen at −80 °C and lyophilized.

The 1H NMR was performed to show the successful methacrylation of gelatin and to determine DS of the final products with different MA modifications according to previous methods [37,71,72] (Fig. S2). The degree of methacrylation of lower MA modification gelatin (GelMA-1) and higher MA modification gelatin (GelMA-2) was determined as 0.138 mmol/g and 0.272 mmol/g by using DMMA as the internal reference.

4.3. Preparation of hydrogels

For physical GelCD hydrogels, Gelatin, ac-β-CD and photo initiator 2-hydroxy-4'-(2-hydroxyethoxy)-2-methylpropiophenone (I2959, Sigma) were dissolved together in PBS at 37 °C to prepare hydrogel precursor with a final concentration of 8% gelatin (w/v), 10% ac-β-CD (w/v) and 0.05% I2959 (w/v). The hydrogel precursor was added into transparent PVC molds and then exposed to 365 nm ultraviolet (UV) light (10 mW/cm^2) for 10 min to form GelCD hydrogels. The preparation of chemical GelMA-1 and GelMA-2 hydrogels was similar. 8% (w/v) of GelMA-1 or GelMA-2 and 0.05% (w/v) of I2959 were dissolved in PBS at 37 °C. The precursor was then added into PVC mold before exposed to 365 nm UV light for 10 min to obtain chemically crosslinked GelMA hydrogels.

4.4. In vitro degradation test

Hydrogel samples were firstly incubated in PBS at 37 °C overnight to reach swelling equilibrium. Afterwards, the weighted samples were placed in 1 mg/mL collagenase solution (type II, ~125 CDU/mg, Sigma) at 37 °C. At predetermined time points (t), hydrogel samples were taken out from collagenase solution and weighed. The degradation rate (DR%) of the hydrogels was determined using Equation (1), where W_0 is the weight of samples after swelling equilibrium and W_t is the weight of samples at time t.

$$DR\% = \frac{W_0 - W_t}{W_0} \times 100\% \quad (1)$$

4.5. Rheological measurements

Rheological characterizations were performed using a Kinexus Rheometer from Malvern. GelCD, GelMA-1 and GelMA-2 hydrogels were first formed in the mold and put into PBS to reach swelling equilibrium before being placed on the Kinexus Rheometer plate. Time sweeps were recorded at a strain of 0.1% and a frequency of 10 Hz with the temperature settled as 37 °C. Frequency sweeps were recorded at a fixed strain of 0.1% and a changing frequency from 0.01 to 10 Hz. For 3-interval time tests, the hydrogel samples underwent sequential shear of 4 cycles with 1% strain for 120 s and 500% strain for 60 s, with a fixed frequency of 1 Hz. During these rheological tests, the storage modulus (G') and the viscous modulus (G") of hydrogel samples were monitored.

4.6. Compression test

The stress relaxation properties of the samples were measured from compression tests of the gel discs (15 mm in diameter, 2 mm thick). The gel discs were compressed to 15% strain with a deformation rate of 0.3 mm s^{-1}. Subsequently, the strain was held constant, while the load was recorded as a function of time.

4.7. 2D mESCs culture

The mESCs named E14 were kindly presented by prof. Bo Feng from the school of Biomedical Sciences, faculty of Medicine, the Chinese University of Hong Kong.

For conditioned 2D culture, according to standard protocol, two most common 2D culture method, namely, 2i method and MEF method, were used. For MEF method, briefly, the mESCs were propagated on inactivated mouse embryonic fibroblast (MEF, Merck) as feeder cells in conditioned culture medium at 37 °C with 5% CO_2. The conditioned medium contains Dulbecco's modified Eagles' medium (DMEM, Gibco) supplemented with 15% mESC-qualified fetal bovine serum (FBS, Millipore), 1 mM L-glutamine (Sigma),1 mM sodium pyruvate (Gibco), 0.1 mM NEAA (Gibco), 50 units of penicillin/streptomycin (Hyclone), 0.1 mM b-mercaptoethanol (Gibco) and 1000 units/mL leukemia inhibitory factor (LIF, Millipore). The medium was changed every day and mESCs were passaged every 2 days onto fresh MEF using TrypLE Express enzyme (Gibco). For 2i method, the overall protocol was similar, except that the mESCs were cultured on gelatin coated culture dish (by incubation of 0.1% gelatin solution from Millipore for at least 1 h) instead of MEF. The medium was the MEF conditioned medium supplemented with extra GSK3β and MEK 1/2 inhibitors (0.1 mM PD03259010 and 0.1 mM CHIR99021 from Santa Cruz, namely, 2i).

4.8. 3D mESCs culture in hydrogel

For 3D hydrogel culture, mESCs were firstly mixed with GelCD or GelMA hydrogel precursors. By using the same procedures of hydrogel preparation, mESCs were encapsulated into hydrogels with the concentration of 1.5×10^5 cells per 50 μl hydrogel. Then cell-laden hydrogels were cultivated in MEF conditioned medium as previously described. The media was changed every day during the culture. For MMP inhibition, the MMP inhibitor, GM 6001 (abcam) was initially added at 50 μM on day 2 and every day thereafter with medium exchanges.

4.9. Cell viability test

Cell viability was assessed by live/dead staining where Calcein AM (Gibco) was used to label living cells with green color and propidium

Iodide (PI, Sigma) was used to label apoptotic cells with red color from day 1 to day 7. Briefly, the mESCs encapsulated hydrogels were rinsed with PBS and then incubated with 4 μM Calcein AM and 10 μg/mL PI in PBS for 20 min. Afterwards, hydrogels were rinsed with PBS for 3 times and observed under confocal microscope.

AlamarBlue assay (Invitrogen) was also used to assess cell viability following the manufacturer's instructions. Briefly, at days 1, 3 and 7, alamarBlue working solution were added to the medium of the mESCs encapsulated hydrogels and then incubated at 37 °C in the incubator. Afterwards, the fluorescent signals (excitation 544 nm, emission 590 nm) were detected. The final data was presented as fluorescent value of each group normalized to the fluorescent value of day 1. All assays were done with three parallel samples.

Cell viability was also assessed using an Annexin V-FITC and 7-AAD Apoptosis Detection Kit (Sino Biological) following the manufacturer's instructions. GelCD and GelMA hydrogels with encapsulated mESC were first degraded using 1 mg/mL collagenase solution at 37 °C for 30 min followed by cell dissociation in TrypLE Express enzyme solution for 5 min. Then, mESCs were collected and resuspended in 100 μL binding buffer. Then 5 μL Annexin V-FITC and 5 μL 7-AAD solution were added. After incubation for 15 min at room temperature in the dark, samples were analyzed with a flow cytometer following supplementary addition of 400 μL binding buffer. All assays were done with three parallel samples.

4.10. Cell proliferation assay

EdU Cell Proliferation Kit with Alexa Fluor 555 (BeyoClick) was used to quantify proliferating mESCs in GelCD and GelMA hydrogels following manufacturer's instructions. Briefly, EdU solution was added to the medium with final concentration of 10 μM 2 h before collecting time point (day 2, day 4 and day 7). Then cell-laden hydrogels were fixed, treated, and stained following the protocol. The proliferating cell fraction (%) was calculated by the number of EdU-positive nucleus divided by the total nucleus in each microscopic horizon in each hydrogel group.

4.11. Immunocytochemistry

For immunocytochemistry, mESCs cultured under 2D conditions or in hydrogels were fixed with 4% paraformaldehyde for 30 min. After permeabilized with 0.25% Triton-X 100 and washed by PBS, samples were incubated with PBS containing 2.5% Bovine Serum Albumin (BSA, Sigma). Then the samples were incubated with primary antibody including SOX2 (1:200, Santa Cruz), OCT3/4 (1:200, Santa Cruz), NANOG (1:400, Abcam), Nestin (1:200, Biolegend), alpha-smooth muscle actin (α-SMA, 1:400, Abcam), alpha-Fetoprotein (AFP, 1:200, R&D system) followed with fluorescence secondary antibodies. Phalloidin-FITC (1:500, Cytoskeleton) was used to stain the cytoskeleton and nuclei were stained with DAPI (1:1000, Sigma). The relative fluorescent intensity of the biomarkers limited to the nuclei area was calculated using ImageJ software.

4.12. Cell morphology analysis

The morphology of mESCs was determined using optical images of the colonies in the hydrogels or on the 2D substrates. The determined area, aspect ratio between long and short axes, and circularity using Equation (2) of the colonies were measured by ImageJ software for quantitative comparison. Ten colonies in each group were randomly selected for the analysis.

$$Circularity = 4\pi \times \frac{Area}{Perimeter^2} \quad (2)$$

4.13. Quantitative RT-PCR

Firstly, samples were homogenized in Trizol reagent (Life Technologies) and total RNA was extracted according to the manufacturer's instructions. The RNA concentration was then determined by ND-100 spectrophotometer (Nanodrop Technologies). RNA from each sample was reverse transcribed into cDNA by RevertAid Fist Strand cDNA Synthesis Kit (Thermo). Quantitative real-time PCR was performed on Applied Biosystems 7300 Real-Time PCR system using Power SYBR Green RT-PCR Kit (Life Technologies. Primer sequences and annealing temperatures are listed in Supplementary Table S1. Results were normalized relative to housekeeping gene PRLP0 by the ΔΔCT relative method.

4.14. EB formation

The mESCs in the GelCD hydrogels were released and harvested by collagenase, dissociated into single cells and transferred to non-adherent culture dishes in the MEF conditioned medium without LIF. Medium was changed every two days. After 3 days, the ESC aggregations were re-plated on the gelatin coated adherent culture dishes and cultured for another 7 days in medium without LIF. The obtained EBs were collected for further immunofluorescence staining with germ layer markers.

4.15. Statistical analysis

All the data are presented as the mean ± SD. Normality of distributions was examined by Shapiro-Wilk test. Data were analyzed by GraphPad Prism software (GraphPad Software Inc.) by conducting unpaired and independent Student's *t*-test for comparison between independent two groups, and one-way ANOVA for comparisons across multiple groups, followed by Tukey's post hoc test. Two-sided $P < 0.05$ was considered statistically significant.

Credit author statement

Xu Xiayi: Conceptualization, Methodology, Resources, Validation, Formal analysis, Investigation, Data curation, Writing – original draft. **Feng Qian**: Conceptualization, Methodology, Resources. **Ma Xun**: Conceptualization, Methodology, Resources. **Deng Yingrui**: Methodology, Resources. **Zhang Kunyu**: Methodology. **Hon Son Ooi**: Methodology, Resources. **Yang Boguang**: Methodology, Resources. **Zhang Zhi-Yong**: Writing – review & editing. **Feng Bo**: Conceptualization, Resources, Writing – review & editing, Funding acquisition. **Bian Liming**: Conceptualization, Resources, Writing – review & editing, Visualization, Supervision, Funding acquisition.

Competing interests

The authors declare that they have no competing interests.

Data and materials availability

All data associated with this study are present in the paper or in the Supplementary Materials.

Declaration of competing interest

The authors declare that they have no known competing financial interests or personal relationships that could have appeared to influence the work reported in this paper.

Data availability

Data will be made available on request.

Acknowledgements

The authors would like to thank Dr. P. Zhao, Dr. X. Yang, Dr. X. Chen, Dr. R. Li, Dr. H. Chen, Dr. C. Yin, Mr. K. Wong, Mr. Z. Li, Mr. X. Xie for participating in valuable discussions. Funding: This project is supported by the National Natural Science Foundation of China (31570979 to L. B.), the Research Grants Council of the Hong Kong Special Adiministration Region (GRF/14202920and grf/14204618 to L. B. and GRF/14119518 to B. F.), and the Health and Medical Research Fund of the Food and Health Bureau of Hong Kong Sepcial Adiminstration Region (08190416 to L. B.).

Appendix A. Supplementary data

Supplementary data to this article can be found online at https://doi.org/10.1016/j.biomaterials.2022.121802.

References

[1] M.J. Evans, M.H. Kaufman, Establishment in culture of pluripotential cells from mouse embryos, Nature 292 (1981) 154–156.
[2] C.E. Murry, G. Keller, Differentiation of embryonic stem cells to clinically relevant populations: lessons from embryonic development, Cell 132 (2008) 661–680.
[3] J.H. Hanna, K. Saha, R. Jaenisch, Pluripotency and cellular reprogramming: facts, hypotheses, unresolved issues, Cell 143 (2010) 508–525.
[4] Self-assembly of embryonic and two extraembryonic stem cell types into gastrulating embryo-like structures, Obstet. Gynecol. Surv. 74 (2019) 30–31.
[5] X. Xue, Y. Sun, A.M. Resto-Irizarry, Y. Yuan, K.M. Aw Yong, Y. Zheng, S. Weng, Y. Shao, Y. Chai, L. Studer, J. Fu, Mechanics-guided embryonic patterning of neuroectoderm tissue from human pluripotent stem cells, Nat. Mater. 17 (2018) 633–641.
[6] O. Lindvall, Z. Kokaia, A. Martinez-Serrano, Stem cell therapy for human neurodegenerative disorders - how to make it work, Nat. Med. 10 (2004) S42–S50.
[7] J.H. Kim, J.M. Auerbach, J.A. Rodriguez-Gomez, I. Velasco, D. Gavin, N. Lumelsky, S.H. Lee, J. Nguyen, R. Sanchez-Pernaute, K. Bankiewicz, R. McKay, Dopamine neurons derived from embryonic stem cells function in an animal model of Parkinson's disease, Nature 418 (2002) 50–56.
[8] C.W. Pouton, J.M. Haynes, Embryonic stem cells as a source of models for drug discovery, Nat. Rev. Drug Discov. 6 (2007) 605–616.
[9] K.A. Johnson, C.P. Lerner, L.C. Di Lacio, P.W. Laird, A.H. Sharpe, E.M. Simpson, Transgenic mice for the preparation of hygromycin-resistant primary embryonic fibroblast feeder layers for embryonic stem cell selections, Nucleic Acids Res. 23 (1995) 1273–1275.
[10] K.G. Chen, B.S. Mallon, R.D. McKay, P.G. Robey, Human pluripotent stem cell culture: considerations for maintenance, expansion, and therapeutics, Cell Stem Cell 14 (2014) 13–26.
[11] A.G. Smith, J.K. Heath, D.D. Donaldson, G.G. Wong, J. Moreau, M. Stahl, D. Rogers, Inhibition of pluripotential embryonic stem cell differentiation by purified polypeptides, Nature 336 (1988) 688–690.
[12] M. Tosolini, A. Jouneau, Acquiring ground state pluripotency: switching mouse embryonic stem cells from serum/LIF medium to 2i/LIF medium, Methods Mol. Biol. 1341 (2016) 41–48.
[13] K. Hayashi, S.M.C. de Sousa Lopes, F. Tang, K. Lao, M.A. Surani, Dynamic equilibrium and heterogeneity of mouse pluripotent stem cells with distinct functional and epigenetic states, Cell Stem Cell 3 (2008) 391–401.
[14] A.M. Singh, T. Hamazaki, K.E. Hankowski, N. Terada, A heterogeneous expression pattern for Nanog in embryonic stem cells, Stem Cell. 25 (2007) 2534–2542.
[15] Y. Toyooka, D. Shimosato, K. Murakami, K. Takahashi, H. Niwa, Identification and characterization of subpopulations in undifferentiated ES cell culture, Development 135 (2008) 909–918.
[16] J. Czyz, A. Wobus, Embryonic stem cell differentiation: the role of extracellular factors, Differentiation 68 (2001) 167–174.
[17] N. Zagris, Extracellular matrix in development of the early embryo, Micron 32 (2001) 427–438.
[18] T.P. Kraehenbuehl, R. Langer, L.S. Ferreira, Three-dimensional biomaterials for the study of human pluripotent stem cells, Nat. Methods 8 (2011) 731–736.
[19] S. Gerecht, J.A. Burdick, L.S. Ferreira, S.A. Townsend, R. Langer, G. Vunjak-Novakovic, Hyaluronic acid hydrogel for controlled self-renewal and differentiation of human embryonic stem cells, Proc. Natl. Acad. Sci. U. S. A. 104 (2007) 11298–11303.
[20] J. Wei, J. Han, Y. Zhao, Y. Cui, B. Wang, Z. Xiao, B. Chen, J. Dai, The importance of three-dimensional scaffold structure on stemness maintenance of mouse embryonic stem cells, Biomaterials 35 (2014) 7724–7733.
[21] J. You, A. Haque, D.S. Shin, K.J. Son, C. Siltanen, A. Revzin, Bioactive photodegradable hydrogel for cultivation and retrieval of embryonic stem cells, Adv. Funct. Mater. 25 (2015) 4650–4656.
[22] S.E. Harrison, B. Sozen, M. Zernicka-Goetz, In vitro generation of mouse polarized embryo-like structures from embryonic and trophoblast stem cells, Nat. Protoc. 13 (2018) 1586–1602.
[23] M. Caiazzo, Y. Okawa, A. Ranga, A. Piersigilli, Y. Tabata, M.P. Lutolf, Defined three-dimensional microenvironments boost induction of pluripotency, Nat. Mater. 15 (2016) 344–352.
[24] A. Ranga, S. Gobaa, Y. Okawa, K. Mosiewicz, A. Negro, M.P. Lutolf, 3D niche microarrays for systems-level analyses of cell fate, Nat. Commun. 5 (2014) 4324.
[25] B. Choi, K.S. Park, J.H. Kim, K.W. Ko, J.S. Kim, D.K. Han, S.H. Lee, Stiffness of hydrogels regulates cellular reprogramming efficiency through mesenchymal-to-epithelial transition and stemness markers, Macromol. Biosci. 16 (2016) 199–206.
[26] A.M. Rosales, K.S. Anseth, The design of reversible hydrogels to capture extracellular matrix dynamics, Nat. Rev. Mater. 1 (2016).
[27] K.Y. Zhang, Q. Feng, J.B. Xu, X.Y. Xu, F. Tian, K.W.K. Yeung, L.M. Bian, Self-assembled injectable nanocomposite hydrogels stabilized by bisphosphonate-magnesium (Mg2+) coordination regulates the differentiation of encapsulated stem cells via dual crosslinking, Adv. Funct. Mater. 27 (2017).
[28] H.Y. Wang, S.C. Heilshorn, Adaptable hydrogel networks with reversible linkages for tissue engineering, Adv. Mater. 27 (2015) 3717–3736.
[29] H. Wang, S.C. Heilshorn, Adaptable hydrogel networks with reversible linkages for tissue engineering, Adv. Mater. 27 (2015) 3717–3736.
[30] O. Chaudhuri, L. Gu, D. Klumpers, M. Darnell, S.A. Bencherif, J.C. Weaver, N. Huebsch, H.P. Lee, E. Lippens, G.N. Duda, D.J. Mooney, Hydrogels with tunable stress relaxation regulate stem cell fate and activity, Nat. Mater. 15 (2016) 326.
[31] S. Khetan, M. Guvendiren, W.R. Legant, D.M. Cohen, C.S. Chen, J.A. Burdick, Degradation-mediated cellular traction directs stem cell fate in covalently crosslinked three-dimensional hydrogels, Nat. Mater. 12 (2013) 458–465.
[32] A.M. Rosales, K.S. Anseth, The design of reversible hydrogels to capture extracellular matrix dynamics, Nat. Rev. Mater. 1 (2016).
[33] K. Zhang, Z. Jia, B. Yang, Q. Feng, X. Xu, W. Yuan, X. Li, X. Chen, L. Duan, D. Wang, L. Bian, Adaptable hydrogels mediate cofactor-assisted activation of biomarker-responsive drug delivery via positive feedback for enhanced tissue regeneration, Adv. Sci. 5 (2018), 1800875.
[34] K.C. Wei, M.L. Zhu, Y.X. Sun, J.B. Xu, Q. Feng, S. Lin, T.Y. Wu, J. Xu, F. Tian, J. Xia, G. Li, L.M. Bian, Robust biopolymeric supramolecular "Host-Guest macromer" hydrogels reinforced by in situ formed multivalent nanoclusters for cartilage regeneration, Macromolecules 49 (2016) 866–875.
[35] O. Chaudhuri, L. Gu, D. Klumpers, M. Darnell, S.A. Bencherif, J.C. Weaver, N. Huebsch, H.P. Lee, E. Lippens, G.N. Duda, D.J. Mooney, Hydrogels with tunable stress relaxation regulate stem cell fate and activity, Nat. Mater. 15 (2016) 326–334.
[36] K.M. Wisdom, K. Adebowale, J. Chang, J.Y. Lee, S. Nam, R. Desai, N.S. Rossen, M. Rafat, R.B. West, L. Hodgson, O. Chaudhuri, Matrix mechanical plasticity regulates cancer cell migration through confining microenvironments, Nat. Commun. 9 (2018).
[37] Q. Feng, K. Wei, S. Lin, Z. Xu, Y. Sun, P. Shi, G. Li, L. Bian, Mechanically resilient, injectable, and bioadhesive supramolecular gelatin hydrogels crosslinked by weak host-guest interactions assist cell infiltration and in situ tissue regeneration, Biomaterials 101 (2016) 217–228.
[38] Q. Feng, J.K. Xu, K.Y. Zhang, H. Yao, N.Y. Zheng, L.Z. Zheng, J.L. Wang, K.C. Wei, X.F. Xiao, L. Qin, L.M. Bian, Dynamic and cell-infiltratable hydrogels as injectable carrier of therapeutic cells and drugs for treating challenging bone defects, Acs Central Sci 5 (2019) 440–450.
[39] C. McKee, G.R. Chaudhry, Advances and challenges in stem cell culture, Colloids Surf. B Biointerfaces 159 (2017) 62–77.
[40] D. Indana, P. Agarwal, N. Bhutani, O. Chaudhuri, Viscoelasticity and adhesion signaling in biomaterials control human pluripotent stem cell morphogenesis in 3D culture, Adv. Mater. 33 (2021), e2101966.
[41] Q. Feng, K. Wei, S. Lin, Z. Xu, Y. Sun, P. Shi, G. Li, L. Bian, Mechanically resilient, injectable, and bioadhesive supramolecular gelatin hydrogels crosslinked by weak host-guest interactions assist cell infiltration and in situ tissue regeneration, Biomaterials 101 (2016) 217–228.
[42] M. Jana, S. Bandyopadhyay, Molecular dynamics study of beta-cyclodextrin-phenylalanine (1:1) inclusion complex in aqueous medium, J. Phys. Chem. B 117 (2013) 9280–9287.
[43] D.B. Bernert, K. Isenbugel, H. Ritter, Synthesis of a novel glycopeptide by polymeranalogous reaction of gelatin with mono-6-para-toluenesulfonyl-beta-cyclodextrin and its supramolecular properties, Macromol. Rapid Commun. 32 (2011) 397–403.
[44] M.F. Ma, S.G. Xu, P.Y. Xing, S.Y. Li, X.X. Chu, A.Y. Hao, A multistimuli-responsive supramolecular vesicle constructed by cyclodextrins and tyrosine, Colloid Polym. Sci. 293 (2015) 891–900.
[45] B.J. Klotz, D. Gawlitta, A. Rosenberg, J. Malda, F.P.W. Melchels, Gelatin-methacryloyl hydrogels: towards biofabrication-based tissue repair, Trends Biotechnol. 34 (2016) 394–407.
[46] K. Yue, G. Trujillo-de Santiago, M.M. Alvarez, A. Tamayol, N. Annabi, A. Khademhosseini, Synthesis, properties, and biomedical applications of gelatin methacryloyl (GelMA) hydrogels, Biomaterials 73 (2015) 254–271.
[47] X. Zhao, Q. Lang, L. Yildirimer, Z.Y. Lin, W. Cui, N. Annabi, K.W. Ng, M. R. Dokmeci, A.M. Ghaemmaghami, A. Khademhosseini, Photocrosslinkable gelatin hydrogel for epidermal tissue engineering, Adv Healthc Mater 5 (2016) 108–118.
[48] T. Lin, C. Chao, S. Saito, S.J. Mazur, M.E. Murphy, E. Appella, Y. Xu, p53 induces differentiation of mouse embryonic stem cells by suppressing Nanog expression, Nat. Cell Biol. 7 (2005) 165–171.
[49] L. Gao, H. Gan, Z.Y. Meng, R.L. Gu, Z.N. Wu, L. Zhang, X.X. Zhu, W.Z. Sun, J. Li, Y. Zheng, G.F. Dou, Effects of genipin cross-linking of chitosan hydrogels on cellular adhesion and viability, Colloids Surf., B 117 (2014) 398–405.
[50] J. Kim, C.M. Hope, N. Gantumur, G.B. Perkins, S.O. Stead, Z.L. Yue, X. Liu, A. U. Asua, F.D. Kette, D. Penko, C.J. Drogemuller, R.P. Carroll, S.C. Barry, G.

G. Wallace, P.T. Coates, Encapsulation of human natural and induced regulatory T-cells in IL-2 and CCL1 supplemented alginate-GelMA hydrogel for 3D bioprinting, Adv. Funct. Mater. 30 (2020).
[51] Y.C. Chen, R.Z. Lin, H. Qi, Y. Yang, H. Bae, J.M. Melero-Martin, A. Khademhosseini, Functional human vascular network generated in photocrosslinkable gelatin methacrylate hydrogels, Adv. Funct. Mater. 22 (2012) 2027–2039.
[52] Y. Wang, M. Ma, J. Wang, W. Zhang, W. Lu, Y. Gao, B. Zhang, Y. Guo, Development of a photo-crosslinking, biodegradable GelMA/PEGDA hydrogel for guided bone regeneration materials, Materials 11 (2018).
[53] C.C. Tang, L.P. Shan, W.M. Wang, G. Lu, R.S. Tare, K.K.H. Lee, Generation of a Bag1 homozygous knockout mouse embryonic stem cell line using CRISPR/Cas9, Stem Cell Res. 21 (2017) 29–31.
[54] F. Chowdhury, Y. Li, Y.C. Poh, T. Yokohama-Tamaki, N. Wang, T.S. Tanaka, Soft substrates promote homogeneous self-renewal of embryonic stem cells via downregulating cell-matrix tractions, PLoS One 5 (2010), e15655.
[55] E.T. Pineda, R.M. Nerem, T. Ahsan, Differentiation patterns of embryonic stem cells in two- versus three-dimensional culture, Cells Tissues Organs 197 (2013) 399–410.
[56] C. McKee, G.R. Chaudhry, Advances and challenges in stem cell culture, Colloids Surf., B 159 (2017) 62–77.
[57] L.S. Ferreira, S. Gerecht, J. Fuller, H.F. Shieh, G. Vunjak-Novakovic, R. Langer, Bioactive hydrogel scaffolds for controllable vascular differentiation of human embryonic stem cells, Biomaterials 28 (2007) 2706–2717.
[58] H. Wang, J. Xiang, W. Zhang, J. Li, Q. Wei, L. Zhong, H. Ouyang, J. Han, Induction of germ cell-like cells from porcine induced pluripotent stem cells, Sci. Rep. 6 (2016), 27256.
[59] R. Zhang, H.K. Mjoseng, M.A. Hoeve, N.G. Bauer, S. Pells, R. Besseling, S. Velugotla, G. Tourniaire, R.E. Kishen, Y. Tsenkina, C. Armit, C.R. Duffy, M. Helfen, F. Edenhofer, P.A. de Sousa, M. Bradley, A thermoresponsive and chemically defined hydrogel for long-term culture of human embryonic stem cells, Nat. Commun. 4 (2013) 1335.
[60] M. Amit, M.K. Carpenter, M.S. Inokuma, C.P. Chiu, C.P. Harris, M.A. Waknitz, J. Itskovitz-Eldor, J.A. Thomson, Clonally derived human embryonic stem cell lines maintain pluripotency and proliferative potential for prolonged periods of culture, Dev. Biol. 227 (2000) 271–278.
[61] C. Wang, R.R. Varshney, D.A. Wang, Therapeutic cell delivery and fate control in hydrogels and hydrogel hybrids, Adv. Drug Deliv. Rev. 62 (2010) 699–710.
[62] C. Fan, D.A. Wang, Macroporous hydrogel scaffolds for three-dimensional cell culture and tissue engineering, Tissue Eng. B Rev. 23 (2017) 451–461.
[63] C. Wang, S. Sinha, X. Jiang, L. Murphy, S. Fitch, C. Wilson, G. Grant, F. Yang, Matrix stiffness modulates patient-derived glioblastoma cell fates in three-dimensional hydrogels, Tissue Eng. 27 (2021) 390–401.
[64] Y. Gong, K. Su, T.T. Lau, R. Zhou, D.A. Wang, Microcavitary hydrogel-mediating phase transfer cell culture for cartilage tissue engineering, Tissue Eng. 16 (2010) 3611–3622.
[65] F.M. Yavitt, T.E. Brown, E.A. Hushka, M.E. Brown, N. Gjorevski, P.J. Dempsey, M. P. Lutolf, K.S. Anseth, The effect of thiol structure on allyl sulfide photodegradable hydrogels and their application as a degradable scaffold for organoid passaging, Adv. Mater. 32 (2020), e1905366.
[66] S. Nam, O. Chaudhuri, Mitotic cells generate protrusive extracellular forces to divide in three-dimensional microenvironments, Nat. Phys. 14 (2018) 621–628.
[67] N. Broguiere, L. Isenmann, C. Hirt, T. Ringel, S. Placzek, E. Cavalli, F. Ringnalda, L. Villiger, R. Zullig, R. Lehmann, G. Rogler, M.H. Heim, J. Schuler, M. Zenobi-Wong, G. Schwank, Growth of epithelial organoids in a defined hydrogel, Adv. Mater. 30 (2018), e1801621.
[68] E.H. Choi, S. Yoon, Y.E. Koh, Y.J. Seo, K.P. Kim, Maintenance of genome integrity and active homologous recombination in embryonic stem cells, Exp. Mol. Med. 52 (2020) 1220–1229.
[69] A.G. Smith, Embryo-derived stem cells: of mice and men, Annu. Rev. Cell Dev. Biol. 17 (2001) 435–462.
[70] N. Sato, I.M. Sanjuan, M. Heke, M. Uchida, F. Naef, A.H. Brivanlou, Molecular signature of human embryonic stem cells and its comparison with the mouse, Dev. Biol. 260 (2003) 404–413.
[71] E. Hoch, C. Schuh, T. Hirth, G.E.M. Tovar, K. Borchers, Stiff gelatin hydrogels can be photo-chemically synthesized from low viscous gelatin solutions using molecularly functionalized gelatin with a high degree of methacrylation, J. Mater. Sci. Mater. Med. 23 (2012) 2607–2617.
[72] A.H. Nguyen, J. McKinney, T. Miller, T. Bongiorno, T.C. McDevitt, Gelatin methacrylate microspheres for controlled growth factor release, Acta Biomater. 13 (2015) 101–110.